

Janus and Ternary Particles Generated by Microfluidic Synthesis: Design, Synthesis, and Self-Assembly

Zhihong Nie, Wei Li, Minseok Seo, Shengqing Xu, and Eugenia Kumacheva*

Contribution from the Department of Chemistry, University of Toronto, 80 Saint George Street, Toronto, Ontario, M5S 3H6 Canada

Received February 6, 2006; Revised Manuscript Received May 17, 2006; E-mail: ekumache@chem.utoronto.ca

Abstract: This paper reports a microfluidic method for fast continuous synthesis of Janus particles and three-phase particles with narrow size distribution. Synthesis of particles included emulsification of monomer liquids and in-situ photoinitiated polymerization of multiphase droplets. We show the strategy for precise control over the structure of Janus particles and their structure-dependent assembly in clusters. We demonstrate an asymmetric chemical modification of the surface of JPs by conjugating them with protein molecules. The Janus and ternary particles were synthesized from largely immiscible liquids and had a sharp interface between the constituent phases.

Introduction

Janus particles (JPs) have long been fascinating objects in the study of self-assembly, in stabilization of emulsions, and as the dual-functionalized optical, electronic, and sensor devices.^{1,2} Janus objects have been obtained from dendrimers,³ block copolymer micelles,⁴ submicrometer-size particles,^{5,6} and micrometer-size beads.^{7–14} Potential applications of Janus particles are determined by the combination of materials building up the hemispheres. For example, particles with oppositely charged hemispheres have a large dipole moment which allows their remote positioning in an electric field.⁷ When loaded with distinct pigments or dyes, the microspheres have potential

applications in the production of color electronic paper.¹⁵ Amphiphilic particles behave as surfactants in stabilization of Pickering emulsions.¹ Janus particles with sharp interface between paired electron donor and acceptor materials can potentially help in converting solar energy into electrical current.

Janus particles have been produced by hydrodynamic techniques,^{6,13} by controlled coalescence of two distinct droplets which was followed by solidification of the merged phases,¹⁶ by phase separation,¹⁸ by using toposelective surface modification,^{7–10,14} template-directed self-assembly,¹⁷ and controlled surface nucleation.¹⁹ Hydrodynamic methods provide a simple single-step, scalable strategy for the preparation of JPs. In particular, synthesis of polymer particles in planar microfluidic reactors proved to be an excellent route to particles with unconventional shapes and morphologies.^{20–22} Two groups have recently reported the preparation of JPs in microfluidic devices

- (1) Perro, A.; Reculusa, S.; Ravaine, S.; Bourgeat-Lami, E.; Duguët, E. *J. Mater. Chem.* **2005**, *15*, 3745–3760.
- (2) Vanakaras, A. G. *Langmuir* **2006**, *22*, 88–93.
- (3) (a) Ropponen, J.; Nummelin, S.; Rissanen, K. *Org. Lett.* **2004**, *6*, 2495–2497. (b) Percec, V.; Imam, M. R.; Bera, T. K.; Balagurusamy, V. S. K.; Peterca, M.; Heiney, P. A. *Angew. Chem., Int. Ed.* **2005**, *44*, 4739–4745.
- (4) (a) Wang, J.; Liu, G.; Rivas, G. *Anal. Chem.* **2003**, *75*, 4667–4671. (b) Erhardt, R.; Zhang, M. F.; Böker, A.; Zettl, H.; Abetz, C.; Frederik, P.; Krausch, G.; Abetz, V.; Müller, A. H. E. *J. Am. Chem. Soc.* **2003**, *125*, 3260–3267.
- (5) Du, Y. Z.; Tomohiro, T.; Zhang, G.; Nakamura, K.; Kodaka, M. *Chem. Commun.* **2004**, *5*, 616–617.
- (6) Roh, K. H.; Martin, D. C.; Lahann, J. *Nat. Mater.* **2005**, *4*, 759–763.
- (7) (a) Cayre, O.; Paunov, V. N.; Velev, O. D. *J. Mater. Chem.* **2003**, *13*, 2445–2450. (b) Cayre, O.; Paunov, V. N.; Velev, O. D. *Chem. Commun.* **2003**, *18*, 2296–2297. (c) Paunov, V. N.; Cayre, O. *J. Adv. Mater.* **2004**, *16*, 788–791.
- (8) Love, J. C.; Gates, B. D.; Wolfe, D. B.; Paul, K. E.; Whitesides, G. M. *Nano Lett.* **2002**, *2*, 891–894.
- (9) Correa-Duarte, M. A.; Salgueirino-Maceira, V.; Rodriguez-Gonzalez, B.; Lizmarzan, L. M.; Kosiorok, A.; Kandulski, W.; Giersig, M. *Adv. Mater.* **2005**, *17*, 2014–2018.
- (10) (a) Takei, H.; Shimizu, N. *Langmuir* **1997**, *13*, 1865–1868. (b) Hugonnot, E.; Carles, A.; Delville, M. H.; Panizza, P.; Delville, J. P. *Langmuir* **2003**, *19*, 226–229.
- (11) Nonomura, Y.; Komura, S.; Tsujii, K. *Langmuir* **2004**, *20*, 11821–11823.
- (12) Velev, O. D.; Lenhoff, A. M.; Kaler, E. W. *Science* **2000**, *287*, 2240–2243.
- (13) Nisisako, T.; Torii, T.; Higuchi, T. *Chem. Eng. J.* **2004**, *101*, 23–29.
- (14) Fujimoto, K.; Nakahama, K.; Shidara, M.; Kawaguchi, H. *Langmuir* **1999**, *15*, 4630–4635.

- (15) (a) Hays, D. A. *J. Electrostatics* **2001**, *51*, 57–63. (b) Sheridan, N. K.; Richley, E. A.; Mikkelsen, J. C.; Tsuda, D.; Crowley, J. M.; Orah, K. A.; Howard, M. E.; Rodkin, M. A.; Swidler, R.; Sprague, R. *Proc. IDRC, SID/IEEE*, Sept. 1997, Toronto, Canada.
- (16) (a) Millman, J. R.; Bhatt, K. H.; Prevo, B. G.; Velev, O. D. *Nat. Mater.* **2005**, *4*, 98–102. (b) Fialkowski, M.; Bitner, A.; Grzybowski, B. A. *Nat. Mater.* **2005**, *4*, 93–97.
- (17) (a) Yin, Y.; Lu, Y.; Xia, Y. *J. Am. Chem. Soc.* **2001**, *123*, 771–772. (b) Yin, Y.; Lu, Y.; Gates, B.; Xia, Y. *J. Am. Chem. Soc.* **2001**, *123*, 8718–8729. (c) Xia, Y.; Yin, Y.; Lu, Y.; McLellan, J. *Adv. Funct. Mater.* **2003**, *13*, 907–918.
- (18) (a) Gu, H.; Zheng, R.; Zhang, X.; Xu, B. *J. Am. Chem. Soc.* **2004**, *126*, 5664–5665. (b) Akiva, U.; Margel, S. *Colloids Surf. A* **2005**, *253*, 9–13.
- (19) (a) Yu, H.; Chen, M.; Rice, P. M.; Wang, S. X.; White, R. L.; Sun, S. *Nano Lett.* **2005**, *5*, 379–382. (b) Reculusa, S.; Poncet-Legrand, C.; Ravaine, S.; Mingotaud, C.; Duguët, E.; Bourgeat-Lami, E. *Chem. Mater.* **2002**, *14*, 2354–2359.
- (20) Jeong, W. J.; Kim, J. Y.; Choo, J.; Lee, E. K.; Han, C. S.; Beebe, D. J.; Seong, G. H.; Lee, S. H. *Langmuir* **2005**, *21*, 3738–3741.
- (21) Dendukuri, D.; Tsoi, K.; Hatton, T. A.; Doyle, P. S. *Langmuir* **2005**, *21*, 2113–2116.
- (22) (a) Xu, S. Q.; Nie, Z. H.; Seo, M.; Lewis, P.; Kumacheva, E.; Stone, H. A.; Garstecki, P.; Weibel, D. B.; Gitlin, I.; Whitesides, G. M. *Angew. Chem., Int. Ed.* **2005**, *44*, 724–728. (b) Nie, Z. H.; Xu, S. Q.; Seo, M.; Lewis, P. C.; Kumacheva, E. *J. Am. Chem. Soc.* **2005**, *127*, 8058–8063. (c) Seo, M.; Nie, Z. H.; Xu, S. Q.; Mok, M.; Lewis, P. C.; Graham, R.; Kumacheva, E. *Langmuir* **2005**, *21*, 11614–11622.

by employing breakup of a liquid thread of two parallel co-flowing streams of monomers or polymer solutions.^{6,13} In both cases, no control of the internal structure or of the surface composition of the microbeads was demonstrated. The counterpart liquids were miscible and the sharpness of interface between the constituent liquids depended on extent of mixing between the adjacent phases before their solidification. Although mixing between liquids undergoing a laminar flow is weak,²³ electrohydrodynamic and hydrodynamic focusing of liquid threads prior to their break up in droplets enhances mixing between the constituent phases and leads to a gradual change in composition along the direction normal to the interface. Formation of particles with gradients in composition can limit some of the applications of JPs (e.g., their use as solar cells systems) in which the existence of a sharp interface between the phases is crucial.

Here, we report continuous microfluidic synthesis of highly monodisperse JPs and ternary polymer particles in the size range from 40 to 100 μm . Production of two-phase and three-phase monomer droplets relied on both thermodynamic and hydrodynamic factors, whereas rapid polymerization allowed trapping of droplet structure in the solid state. The present work reports the following new features: (i) a strategy for precise control over the structure of Janus particles and their structure-dependent assembly in clusters; (ii) an asymmetric chemical modification of the surface of JPs; (iii) the preparation of ternary (three-phase) particles in a microfluidic reactor; and (iv) the synthesis of JPs from largely immiscible liquids and hence production of particles with a sharp interface between the constituent phases.

Results and Discussion

We generated Janus droplets in a microfluidic flow-focusing device (MFFD)²⁴ fabricated in a polyurethane (PU) elastomer by using soft-lithography.²⁵ In the schematic of Figure 1a two liquid monomers (M1 and M2), each mixed with a photoinitiator, are supplied to two central channels of the MFFD. An aqueous 2.0 wt % solution of sodium dodecylsulfate, SDS, (W) is injected to the side channels of the MFFD. At the exit from the central channels the monomers form a two-liquid thread that is forced through a narrow orifice. Under the action of shear imposed by the continuous phase, the thread breaks up to release Janus droplets. Here, the breakup of the thread occurred in the flow-focusing regime.^{22c,24} The droplets were exposed to UV-irradiation in the downstream channel, as well as in the extension wavy channel with a length ca. 200 mm.

Figure 1b shows a typical optical microscopy image of the formation of Janus droplets in the PU MFFDs. We used methacryloxypropyl dimethylsiloxane as M1 and a mixture of pentaerythritol triacrylate (45.0 wt %), poly(ethylene glycol) diacrylate (45.0 wt %) and acrylic acid (5.0 wt %) as M2. Both M1 and M2 contained 4 \pm 1 wt % of 1-hydroxycyclohexyl phenyl ketone. The properties of monomers are provided in Supporting Information.

In the present work, the Reynolds number, Re, and the Capillary number, Ca, of the monomer phase (Re_{drop} , Ca_{drop})

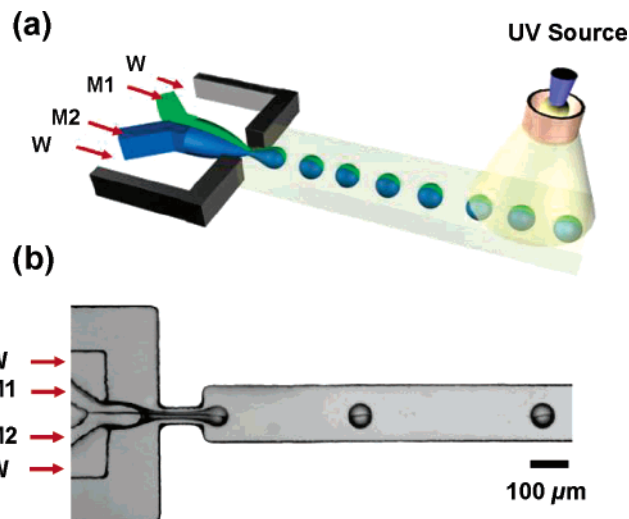


Figure 1. (a) Schematic of generation of Janus droplets from immiscible monomers M1 and M2, emulsified in an aqueous solution of SDS (W). The droplets are irradiated with UV light in the downstream channel. (b) Optical microscopy image of formation of Janus droplets. Flow rates of M1, M2, and W are 0.02, 0.02, and 4 mL/h, respectively. The height of the MFFD is 120 μm and the orifice width is 60 μm . The scale bar is 100 μm .

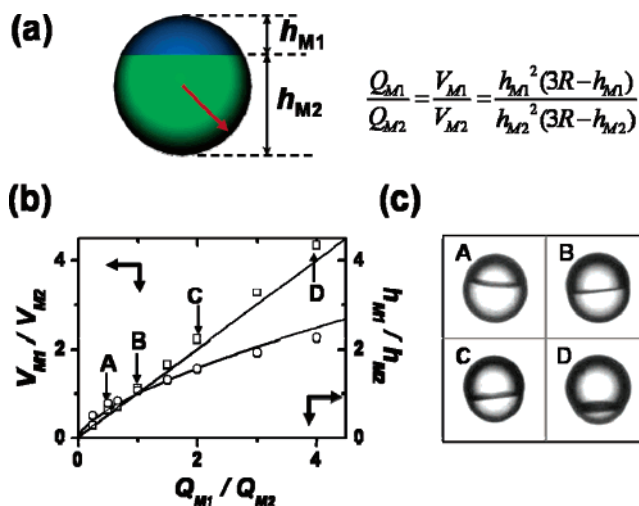


Figure 2. (a) Schematic of Janus droplet and relationship between the ratio of monomer flow rates (Q_{M1}/Q_{M2}) and the ratio of volumes (V_{M1}/V_{M2}) and the ratio of heights (h_{M1}/h_{M2}) of the constituent parts in Janus droplets; (b) Variation in volume ratio V_{M1}/V_{M2} (\square) and height ratio h_{M1}/h_{M2} (\circ) plotted vs the ratio of flow rates of M1 and M2. The solid lines represent calculated theoretical calculations; the empty symbols correspond to experimental results. (c) Optical microscopy images of droplets obtained under conditions indicated in (b) as A, B, C, and D, respectively. The top part of droplets is formed by M1.

and the continuous phase (Re_{drop} , Ca_{cont}) varied in the range of $4 \times 10^{-3} \leq \text{Re}_{\text{drop}} \leq 0.06$, $0.02 \leq \text{Ca}_{\text{drop}} \leq 0.60$ and $1.0 \leq \text{Re}_{\text{cont}} \leq 35$, $4 \times 10^{-3} \leq \text{Ca}_{\text{cont}} \leq 0.40$.²⁰ By changing the ratio of flow rates of M1, M2, and W, we achieved good control over the volume, V , of Janus droplets and the fraction of each liquid in the droplets. The value of V changed as $V \sim (Q_{M1} + Q_{M2})/Q_W$, where Q_W , Q_{M1} , Q_{M2} are the flow rates of W, M1, and M2, respectively. By changing the values of Q_{M1} and Q_{M2} from 0.01 to 0.1 mL/h and the value of Q_W from 0.4 to 12 mL/h, we obtained Janus droplets with diameters from 40 to 100 μm .

Figure 2a–c shows the strategy for controlling the volume fractions of the constituent liquids in Janus droplets with an approximately flat interface between the adjacent phases.

(23) Squires, T. M.; Quake, S. R. *Rev. Mod. Phys.* **2005**, *77*, 977–1026.

(24) (a) Anna, S. L.; Bontoux, N.; Stone, H. A. *App. Phys. Lett.* **2003**, *82*, 364–366. (b) Garstecki, P.; Stone, H. A.; Whitesides, G. M. *Phys. Rev. Lett.* **2005**, *94*, 164501/1–4.

(25) Xia, Y.; Whitesides, G. M. *Angew. Chem., Int. Ed. Engl.* **1998**, *37*, 550–575.

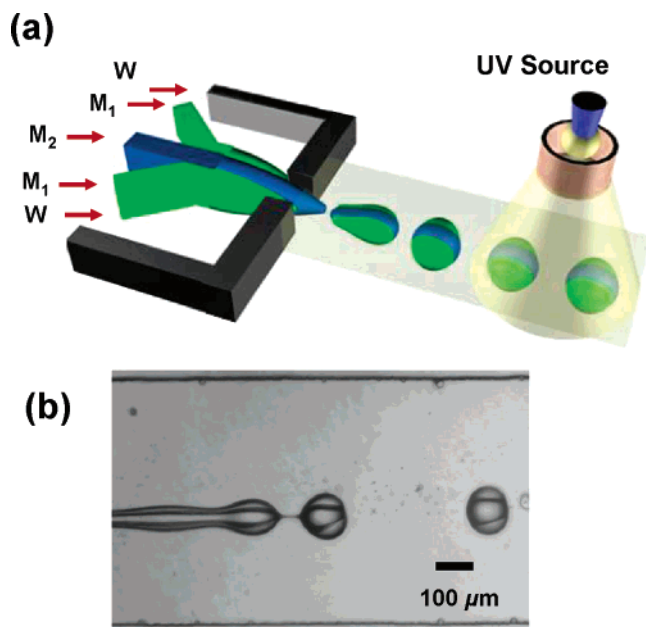


Figure 3. (a) Schematic of formation of droplets with ternary structures. (b) Optical microscopy image of the generation of droplets with a ternary structure. Monomers M1 and M2 are introduced in intermediate and central channels, respectively. Flow rates of M1, M2, and W were 0.16, 0.2, and 16 mL/h, respectively.

Assuming that each phase formed a truncated sphere, a simple relationship was derived that related the ratio of flow rates Q_{M1}/Q_{M2} to the ratio of volumes in an individual droplet, V_{M1}/V_{M2} (or to the ratio of heights of each hemisphere h_{M1}/h_{M2}) (Figure 2a), where R is the radius of the Janus droplet, given by

$$\frac{Q_{M1}}{Q_{M2}} = \frac{V_{M1}}{V_{M2}} = \frac{h_{M1}^2(3R-h_{M1})}{h_{M2}^2(3R-h_{M2})} \quad (1)$$

Figure 2b shows good agreement between the experimental and predicted variation in V_{M1}/V_{M2} (and h_{M1}/h_{M2}) with increasing ratio of monomer flow rates, Q_{M1}/Q_{M2} . The representative morphologies of Janus droplets with volume ratios of monomer phases of 2/1, 1/1, 1/2, and 1/4 (corresponding to the points A, B, C, and D in Figure 2b) are shown in Figure 2c. We note that for $V_{M1}/V_{M2} > 4$ or $V_{M2}/V_{M1} > 4$ the droplets acquired an eyeball shape (image D, Figure 2c): the phase with a larger volume tend to acquire a spherical shape, thus distorting the overall shape of the Janus droplet. This effect explained the difference between experimental and theoretical values of V_{M1}/V_{M2} and h_{M1}/h_{M2} in Figure 2b for the large difference in volume of two compartments of the droplets.

We also obtained droplets with a ternary structure by introducing M2 in the central channel, M1 in the intermediate channels and an aqueous SDS solution in the side channels, as shown in the schematic of Figure 3a. In contrast with Janus droplets, ternary droplets could be obtained only in the jetting regime^{22c} when a liquid thread of three parallel co-flowing monomer streams extended to more than five orifice widths (Figure 3b).

Morphology of Janus and ternary droplets was governed by the combination of hydrodynamic and thermodynamic factors. Formation of droplets with Janus and three-phase structures critically depended on the values of interfacial energies between the liquids (characterized by the spreading coefficient, S_i , of

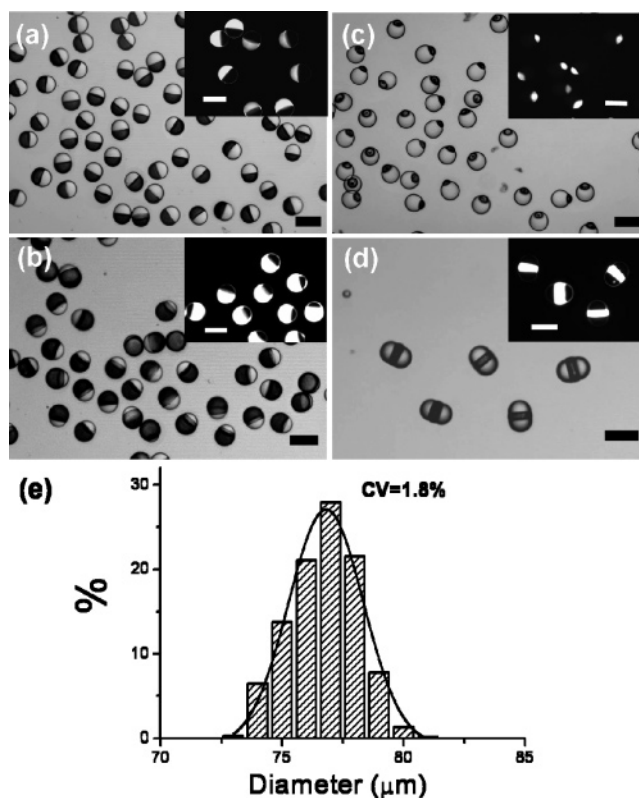


Figure 4. Optical microscopy images of JPs (a–c) and particles with ternary structures (d). Bright and dark phases are polymers of M1 and M2, respectively. Insets in (a–d) show fluorescence microscopy images of the corresponding particles (bright phase is a polymer of M2 mixed with NBD-MA dye). Flow rates of M1, M2 and W in each channel are, mL/h: (a) 0.02, 0.02, 1.5; (b) 0.01, 0.03, 1.5; (c) 0.04, 0.008, 2; (d) 0.14, 0.16, 10. (e) Size distribution of particles shown in (a). CV = 1.8%.

each phase). The value of S_i was defined as $S_i = \sigma_{jk} - (\sigma_{ij} + \sigma_{ik})$,²⁷ where the subscripts i, j, k represented M1, M2, and W, respectively, without repetition; and σ was the value of interfacial tension between the two subscripted phases. In our work, the values of S_{M1} , S_{M2} , and S_W were -3.66 , 1.38 , and -6.12 mN/m, respectively. For $S_w > 0$ ($S_{M1} < 0$, $S_{M2} < 0$), phase separation occurred: two “halves” of the Janus droplet did not adhere to each other and produced individual droplets.

Ternary droplets formed only when M1 (the monomer with a lower value of S_i) was introduced in the intermediate channels (as in Figure 3): if M1 was supplied to the central channel, the side streams of M2 merged at the tip of the liquid thread and engulfed the core of M1. The relative affinity of the monomers to the surface of MFFD played a crucial role in the formation of ternary droplets: monomer M1, the liquid with a lower affinity to the surface of MFFD, was injected in the intermediate channels. Finally, the ratio of flow rates of monomers determined their volume fractions in Janus and ternary droplets: for example, different ternary structures in Figure 3b and Figure 4d originated from the difference in the ratio of flow rates of M1 and M2.

Ternary droplets and Janus droplets with different volume fractions of M1 and M2 were solidified by in-situ photoinitiated

(26) (a) Jeon, N. L.; Baskaran, H.; Dertinger, S. K. W.; Whitesides, G. M.; Van de Water, L.; Toner, M. *Nat. Biotechnol.* **2002**, *20*, 826–830. (b) Dertinger, S. K. W.; Chiu, D. T.; Jeon, N. L.; Whitesides, G. M. *Anal. Chem.* **2001**, *73*, 1240–1246.

(27) Torza, S.; Mason, S. G. *Science* **1969**, *163*, 813–814.

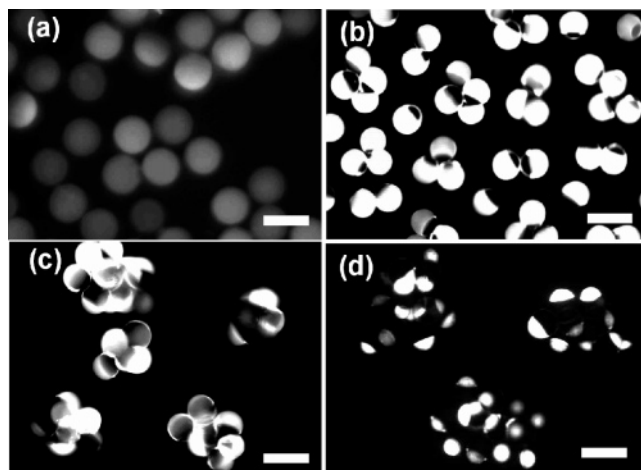


Figure 5. (a) Fluorescent microscopy image of amphiphilic Janus particles at the water-silicone oil interface. A fluorescent hydrophobic phase is immersed in the top oil phase (density 0.8 g/cm^3). (b–d) Clusters of JPs with V_{M1}/V_{M2} of 1/3, 1/1, and 4/1, respectively, in a 92/8 v/v water–methanol mixture. Bright and dark phases are polymers of M1 and M2, respectively. Scale bar is $100 \mu\text{m}$.

free-radical polymerization. Fast polymerization of multiphase droplets allowed one to trap the structures of droplets in the solid state. Typically, the time before polymerization was from 1.5 to 40 ms and the exposure time of droplets to UV-irradiation (400 W , $\lambda = 330\text{--}380 \text{ nm}$) in the microfluidic device was from 2 to 50 s. Figure 4a–c shows bright-field optical microscopy images of monodisperse ($2.8\% < \text{CV} < 4.7\%$) JPs obtained from the droplets with volume ratios of monomers 1/1, 1/3, and 4/1, respectively. Insets in Figure 4a–c show fluorescence microscopy images of the corresponding particles. Contrast between the phases was achieved by introducing a small amount of fluorescent monomer NBD-methacrylate (NBD-MA) in M2. Figure 4d shows a bright-field optical and fluorescence (inset) microscopy image of ternary particles with the aspect ratio 1.45. Typically, the volume ratio of M1 to M2 in ternary particles varied from 1/2 to 2/1. All particles had a sharp interface between the phases.

The Janus particles obtained in the present work were amphiphilic: the contact angles of water on polymer films derived from M1 and M2 were 116.5° and 57.1° , respectively. As a result of their amphiphilic nature, the microspheres underwent self-assembly at the water–oil interface with a hydrophilic part immersed in the water and a hydrophobic part immersed in the oil (Figure 5a).

Furthermore, in the homogeneous liquid medium JPs formed clusters with an aggregation number determined by the ratio of volume fractions of the hydrophilic and hydrophobic parts in the microbeads. Figure 5b–d shows exemplary images of clusters of JPs obtained in the 92/8 v/v water–methanol mixture. Extent of aggregation increased with increasing fraction of the hydrophobic part in the particle: the average aggregation number of particles in these clusters was 2.5, 6, and 11.5 for the JPs with V_{M1}/V_{M2} of 1/3, 1/1, and 4/1, respectively. This trend correlated with the simulations performed by Moncho-Jorda et al.²⁸ who showed that the probability of forming adhesive contacts by colloidal particles depends on the fraction

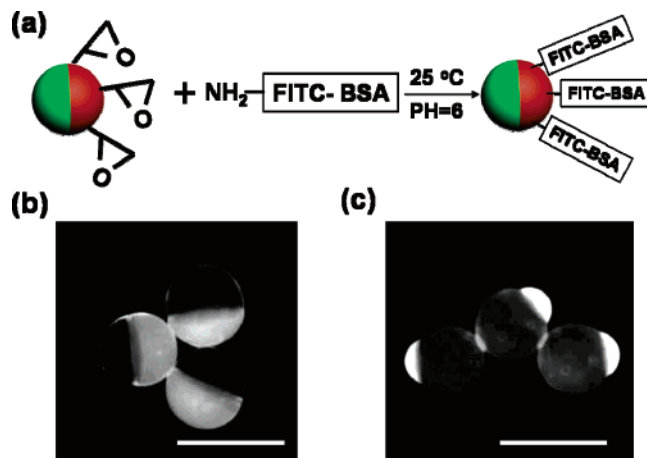


Figure 6. Selective functionalization of Janus particles with FITC–BSA. (a) Schematic of the reaction of bioconjugation. (b,c) Janus particles with different volume fractions of a hydrophilic phase asymmetrically bioconjugated with FITC–BSA. Bright phase: polymer obtained by polymerizing pentaerythritol triacrylate mixed 16 wt % of glycidyl methacrylate. Scale bar is $100 \mu\text{m}$. $\lambda_{\text{exc}} = 495 \text{ nm}$.

of particle surface covered with bridging groups. The results shown in Figure 5b–d suggest a route to new types of self-assembled structures that are realized by designing colloid particles with a controlled fraction of the aggregating constituent.

Polymer Janus particles described in the present work carried different surface functionalities: a hydrophilic compartment of the microspheres contained carboxylic groups introduced by mixing M1 with acrylic acid. Furthermore, JPs could serve as the carriers of different functionalities bound to the surfaces of the microbeads *after* microfluidic synthesis. Here, we demonstrated a highly selective functionalization of JPs by conjugating their hydrophilic compartment with bovine serum albumin (Figure 6). We introduced epoxy groups in the hydrophilic phase of JPs: microbeads carrying surface epoxy groups are ideal systems for protein immobilization via reactions with nucleophilic groups of proteins (e.g., amino, hydroxyl, or thiol moieties) that is accomplished with minimal chemical modification of the protein.²⁹ We synthesized a hydrophilic part of JPs from pentaerythritol triacrylate mixed 16 wt% of glycidyl methacrylate; the hydrophobic phase was synthesized from a methacryloxypropyl dimethylsiloxane. The Janus droplets were generated in the 2 wt% SDS aqueous solution at $\text{pH} = 6$. The epoxy groups were stable on the time scale of microfluidic experiment. Following polymerization of Janus droplets, we attached bovine serum albumin covalently labeled with fluorescein isothiocyanate (FITC–BSA) to the surface of Janus particles, as shown in Figure 6a. The reaction was carried out for 3 h at r.t. at $\text{pH} = 6$. Figure 6b,c shows typical fluorescence microscopy images of asymmetrically bioconjugated Janus particles with different fractions of hydrophilic and hydrophobic compartments. The method allowed control over the surface area carrying bovine serum albumin by changing the volume ratio of surface area of each phase on Janus particles.

(28) Moncho-Jorda, A.; Odriozola, G.; Tirado-Miranda, M.; Schmitt, A.; Hidalgo-A'lvarez, R. *Phys. Rev. E: Stat. Phys., Plasmas, Fluids* **2003**, *68*, 011404.

(29) (a) Chen, J. P.; Chu, D. H.; Sun, Y. M. *J. Chem. Technol. Biotechnol.* **1997**, *69*, 421–428. (b) Mateo, C.; Torres, R.; Fernández-Lorente, G.; Ortiz, C.; Fuentes, M.; Hidalgo, A.; López-Gallego, F.; Abian, O.; Palomo, J. M.; Betancor, L.; Pessela, B. C. C.; Guisan, J. M.; Fernández-Lafuente, R. *Biomacromolecules* **2003**, *4*, 772–777.

Conclusion

In summary, we demonstrated microfluidics-based synthesis of Janus particles and three-phase particles with a sharp interface between the constituent phases and precise control over the structure and size distribution of microbeads. We showed that amphiphilic JPs with different volume fractions of the constituent phases form clusters with different aggregation numbers. We selectively functionalized the surface of JPs during microfluidic synthesis by introducing functional moieties in one of the monomer phases or by conducting asymmetric bioconju-

gation of Janus particles with covalently attached bovine serum albumin after microfluidic synthesis.

Acknowledgment. The authors thank NSERC for supporting this work through the Canada Research Chair program.

Supporting Information Available: Description of design and fabrication of microfluidic devices and of properties of monomers. This material is available free of charge via the Internet at <http://pubs.acs.org>.

JA060882N